Gradual broadening of successive above-threshold-ionization peaks

L. A. A. Nikolopoulos[1] and P. Maragakis[2]

[1]*Institute of Electronic Structure and Laser, P.O. Box 1527, Heraklion-Crete 71110, Greece*
[2]*Division of Engineering and Applied Sciences, Harvard University, 02138 Cambridge Massachusetts*

We present theoretical calculations that show a systematic increase of the spectral widths of the successive above-threshold-ionization (ATI) peaks using Fourier-limited pulses. The increase of the width is attributed to the effective Fourier width corresponding to the higher-order processes. Based on that interpretation, we propose a simple model of calculating the width of a Nth-order ATI peak. We compare the results obtained from this model to the results obtained through the direct propagation of the time-dependent Schrödinger equation. For this, we have selected the negative hydrogen ion that represents the simplest possible system to study this feature due to the absence of resonances, that may obscure the results. Considering that Fourier-limited laser pulses with duration of the order of few tens of fs and wavelengths around the optical regime are nowadays readily available, we address the question about the nature of the photoelectron energy spectrum when the atoms are exposed in such fields.

I. INTRODUCTION

The interaction of an atom with an intense laser pulse inevitably leads to the sequential stripping of the electrons of the atom during the rise of the pulse, as has been proposed by Lambropoulos [1]. This demonstrates the difficulty of exposing an atom to a high-intensity laser field. During the past decade the advances in laser technology focused both on increasing the maximal intensity and on shortening the duration of the laser pulses. Nowadays, laser intensities routinely overcome the atomic unit of intensity, and pulses as short as 10 fs are available in the optical and near-infrared spectral ranges. Recently, XUV/x-ray pulses of duration of 1–2 fs or subfemtoseconds have been reported in the literature [2,3].

The pulsed nature of the field allows the atom to experience the maximum intensity before complete ionization occurs. A rich source of information concerning the interaction of a laser pulse with an atom is provided by the spectrum of the free-electrons generated from this interaction. This spectrum, called the above-threshold-ionization (ATI) spectrum, exhibits a characteristic peaked structure, with the series of peaks separated by energies of a single photon [4]. The systematic collection and analysis of the ATI spectra in short-laser pulses has reached some maturity at the present time, at least for the single-electron ionization case.

Freeman *et al.* [5] measured the dynamic resonances with the Rydberg states whose images are imprinted in the ATI spectrum. This is by now a standard experimental as well as theoretical tool that helps in the characterization of substructures separated from the main peaks. The interaction of multielectron atoms with lasers may reveal similar substructures in the ATI spectrum, due to the larger number of open channels available to the outgoing electron [6–8]; these features, however, are not related to the duration of the pulse. The shift of the photoelectron spectrum with the ponderomotive energy is also well understood. Recently the modeling of the ionization process with large ponderomotive shifts was used to obtain absolute values of multiphoton ionization cross sections in rare gases [9,10]. Bardsley *et al.* [11] predicted a series of subpeaks at the side of the main ATI peaks due to interferences of outgoing continuum wave packets generated at different cycles of the pulse. With the availability of Fourier-limited laser pulses with very-short durations, phenomena that up to now could only be predicted with the use of time-dependent theories for the single-atom response should soon become experimentally feasible. One of the most prominent anticipated measurements is the asymmetry in the angular distribution of the ATI electrons [12]. This occurs due to the initial phase of the laser pulse, that leads to the breaking of the symmetry between up and down with respect to the polarization axis of a linearly polarized laser field. A similar effect was recently proposed by Corkum [13] for a circularly polarized laser pulse. The idea, in this case, is that a single-shot experiment will display a strong angular asymmetry depending on the orientation of the electric-field vector at the time that the field reaches its maximum. It is expected that measurements of this type will characterize the initial phase of ultrashort, few-cycle pulses, once these pulses are available at high-enough intensities and relatively stable conditions.

In this work, we propose that the gradual broadening of successive ATI peaks is a feature of the interaction of Fourier-limited laser pulses with atoms, and present a simple model that predicts this broadening, with high accuracy. Ruling out the Freeman and Bardsley resonances, the effect of the ponderomotive shifts on the shape of the top of the ATI peaks and considering ionization widths that are smaller than the Fourier width of the pulse, the main contribution to the ATI peaks width is the Fourier width of the pulse itself. The ponderomotive shift can be controlled by changing the maximum intensity of the pulse. The Bardsley fringes depend strongly on the duration of the pulse, but as we will see, in most cases they are not relevant in what we will discuss. Freeman resonances are best ruled out by avoiding them. This can be accomplished either by carefully choosing the laser parameters so as to be off resonant during the entire pulse, or by choosing a system that does not have any bound excited states such as the negative hydrogen ion. This system

has attracted much experimental [14–16] and theoretical [17–21] interest recently. Especially, in Ref. [18], Telnov and Chu, through an adiabatic approach, focus on the study of shape effects of long length (picosecond pulses on the multiphoton photoelectron energy distribution of the detached electron in the wavelength of 1064 nm). In this work, we address a feature of the photoelectron energy spectrum that is most prominent in the opposite extreme, regarding the duration of the pulse.

Atomic units have been used in the calculations, however, in the presentation and the figures we cite wavelengths in nm, energies in eV and intensities in W/cm^2 (1 a.u. of intensity is 3.51×10^{16} W/cm^2).

II. METHOD

For the results that follow we have chosen the negative hydrogen ion because of the clarity of its ATI spectrum that is free from resonant effects that may obscure the features we discuss. For the reasons of experimental convenience it would most likely be simpler to study a different system in an experiment. We solve the time-dependent Schrödinger equation (TDSE), both using a correlated two-electron method [20] and using a single-active electron approach with a Yukawa potential. The techniques that we use for the numerical solution of the TDSE have been reviewed in [8]. We will briefly highlight the main points of these techniques. All equations that follow are given in atomic units.

The TDSE for an atomic system in an external laser field is written as

$$i\partial_t \psi(t) = [H_0 + V_I(t)]\psi(t), \quad (1)$$

with H_0 the field-free atomic Hamiltonian and V the time-dependent interaction between the system and the laser field. In the length gauge and within the dipole approximation, the interaction operator is $V_I(t) = -\mathbf{r}\cdot\mathbf{E}(t)$, where $\mathbf{r} = \mathbf{r}_1 + \mathbf{r}_2$ is the position vector of the active electrons of the system and $\mathbf{E}$ the electric field. In our calculations, we assume laser fields linearly polarized along the z axis with

$$\mathbf{E}(t) = \mathbf{e}_z E_0 f(t)\sin\omega t, \quad -\frac{T}{2} < 0 < \frac{T}{2}, \quad (2)$$

where $f(t) = \cos^2(\pi t/T)$ is the pulse envelope of total duration T for a field of angular frequency ω. We have chosen the cos^2 profile instead of a Gaussian profile because of its finite duration, that is best suited for numerical integration.

In our two-electron calculations we expand the time-dependent wave function onto a stationary eigenbasis constructed within a box, an approach that has been used in calculations of the ATI spectrum of the negative hydrogen ion [20]:

$$\psi(t) = \sum_{n\Lambda} C_n^\Lambda(t)\Phi_{E_n}^\Lambda + \sum_\Lambda \int C_E^\Lambda(t)\Phi_E^\Lambda dE, \quad (3)$$

where $\Lambda \equiv (SLM_L M_S)$ denotes the angular-quantum-numbers characterizing LS-uncoupled eigenstates of the system. Given that the ground state of the negative hydrogen ion

is an $^1S_0$ state and considering that for linearly polarized light and dipole allowed transitions, $\Delta S = 0, \Delta M_L = 0$, only the singlet $M_L = M_S = 0$ states need to be included in the expansion of the time-dependent wavefunction $\psi(t)$.

The basic idea and the formal details of the construction of the two-electron states (with total angular momentum L) can be found in [22]. We obtain the two-electron states $\Phi_{n(E)}^{SL}$ by diagonalizing the Hamiltonian in the basis spanned by two-electron basis functions $\Psi_{n_1 l_1, n_2 l_2}^{SL}(\mathbf{r}_1, \mathbf{r}_2)$, constructed as an antisymmetrized product of one-electron hydrogen orbitals. The radial part of the one-electron orbitals is expanded on a set of 992 B splines of order $k = 9$ inside a finite interval $[0,R]$, with R up to 1000 a.u. The two-electron basis functions $\Psi_{n_1 l_1, n_2 l_2}^{SL}(\mathbf{r}_1, \mathbf{r}_2)$ are constructed in terms of about 2000 configurations $(n_1 l_1, n_2 l_2)$ for the symmetry $L = 0$ and about 1500 for each of the other symmetries up to $L = 8$. Inserting the expansion (3) into the TDSE we obtain a system of ordinary differential equations (ODE) for the coefficients $C_{E_n}^L(t)$,

$$i\frac{d}{dt}C_{E_n}^L(t) = C_{E_n}^L(t)E_n + \sum_{L',E_n'} (\Phi_{E_n}^{L'}|V_I(t)|\Phi_{E_n'}^{L'})C_{E_n'}^{L'}(t). \quad (4)$$

Integration of the above system of differential equations, subject to the proper initial conditions provides the coefficients at the end of the pulse and thus, for our chosen pulse profile, at $t \to \infty$.

In addition, for reasons of numerical efficiency, we performed calculations using the single-active-electron approach with a Yukawa potential: $V(r) = -V_0 \exp(-\beta r)/r$, with $V_0 = 1.1$ and $\beta = 1$, which reproduces the qualitative features of the negative hydrogen ion and has been applied to the study of this system [23,24]. The resulting three-dimensional time-dependent wave function is expanded on a set of spherical harmonics and radial B splines that leads to a set of ODE for the time-dependent coefficients. The details of the relevant techniques can be found in the review by Lambropoulos et al. [8], as well as in the work by Maragakis et al. [25], as they have been applied to the study of Potassium in the presence of mid-infrared radiation.

In our calculations we have used a box of 2000 a.u., with 2000 B splines of order 7 for each of the 16-lowest angular momenta. On the one hand, this method allows us to obtain more ATI peaks using a larger box, while on the other hand, it provides an additional test of our model.

In both cases, convergence of the results have been checked against the radius box as well as in the total number of states included in the basis.

III. RESULTS AND DISCUSSION

In the top part of Fig. 1, we present the photoelectron energy spectrum of the negative hydrogen ion as calculated using the two-electron basis-expansion technique, at a wavelength of 1064 nm (1.165 eV), intensity of 10^{11} W/cm^2, using a cos^2 pulse profile with a full width at half maximum (FWHM) of 28.4 fs. The total-pulse duration corresponds to
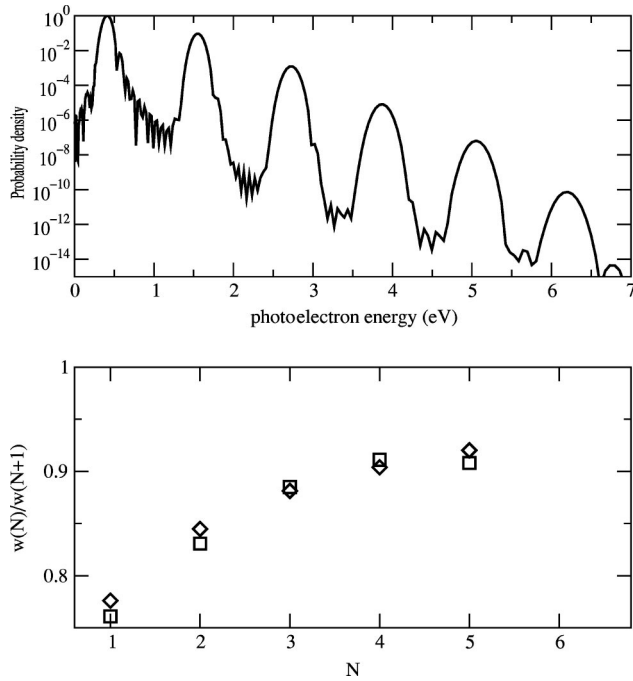
FIG. 1. The top figure shows the ATI spectrum (in eV^{-1}) of the negative hydrogen-ion irradiated by a 28-fs pulse with peak intensity of 10^{11} W/cm^2 and wavelength of 1064 nm. The bottom figure displays the ratio of the widths of successive ATI peaks. The square boxes are obtained from the calculated spectra and the diamonds are the values predicted by the model.

16 optical cycles of the field. The energy of the photon is sufficient to ionize the negative-hydrogen ground state with a single photon. The first peak shown in the figure corresponds to a single-photon ionization process. Note the Bardsley fringes on the right-hand side of the peak. The y axis is on a logarithmic scale and thus it is clear that the side peaks do not affect the width of the first peak significantly. Measuring the widths of the successive peaks we obtain 0.102 eV, 0.134 eV, 0.164 eV, 0.183 eV, 0.200 eV, and 0.221 eV, respectively, for the peaks of order 1, 2, 3, 4, 5, and 6. We have given an explanation of this significant broadening within a perturbative framework. The first peak corresponds to a single-photon absorption, thus the ionization rate is proportional to the first power of intensity. The ion experiences a cos^2 pulse profile whose Fourier width, inversely proportional to its FWHM, will contribute to the broadening of this peak. On the other hand, the Nth order peak results from the absorption of N photons, thus the ionization rate is proportional to the Nth power of the intensity, and the peak is generated by an effective cos^{2N} pulse profile. This pulse is more sharply peaked than the fundamental field, thus its width is less, resulting in a broader Fourier width. In other words, for a Nth-order process the effective time interaction between the atom and light, defined as [26]

$$T_{\mathrm{eff}}^{(N)} = \int_0^t dt' f^N(t'),\qquad(5)$$

is the quantity that determines the spectral width of the Nth-order process.

For example, more accurately, taking the Fourier transform of the Nth power of the field,

$$\hat{E}^{(N)}(\omega) = \int_{T/2}^{-T/2} dt E^N(t) e^{i\omega t},\qquad(6)$$

we obtain for the case of a Gaussian pulse profile (of duration T), that the temporal width contributing to the Nth-order process equals to $2\sqrt{\ln 2}/\sqrt{N}$. The corresponding spectral width, and thus the Nth-order peak width $w(N)$, is proportional to the square root of the order of process:

$$w(N) = |\hat{E}^{(N)}(\omega_+) - \hat{E}^{(N)}(\omega_-)| \sim \sqrt{N},\qquad(7)$$

where, the frequencies $\omega_\pm$, are defined through the relation, $\hat{E}^{(N)}(\omega_\pm) = \hat{E}_{\mathrm{max}}^{(N)}/2$, with $\hat{E}_{\mathrm{max}}^{(N)}$, being the peak value of $\hat{E}^{(N)}(\omega)$. It is clear from the latter expression that the spectral width of the ATI peaks is an increasing function of the order of the process. This feature is characteristic for any Fourier-limited pulse, whatever the temporal shape of the field.

Turning now again to the calculations, where we have used cos^2 pulse, we make a comparison with the calculated ATI spectrum. For this we define the quantity $w(N)/w(N+1)$, which gives the ratio of the width of the Nth peak to the width of the $(N+1)$th peak. The bottom part of Fig. 1 shows a comparison of the peak-width ratios predicted by the Eq. (6) and (7) to the ratios obtained from the numerical simulation; the agreement is very good. The numerical simulation is converged up to 7 eV because of the limitations entering the basis method, thus only the first-five ratios are shown. The Fourier widths of the cos^2 pulse-profile envelope have been calculated numerically. If we had done the estimate based on the inverse of the temporal width of the corresponding pulse profile [see Eq. (5)], the disagreement in the first ratio would be somewhat larger.

According to the model, the broadening of the peaks does not depend on the number of electrons of the atom, as long as we are within the single-electron response regime. We have performed a supplementary series of calculations, using this time the Yukawa potential to model the negative hydrogen ion. This results to a single-active electron response of the problem, thus allows us to enlarge the range of convergence of our results. The broadening of the successive ATI peaks is observed in all calculations that we performed and agrees quite well with the model. As a representative example, in Fig. 2 we present the ATI spectrum at 1519 nm (0.816 eV), 5×10^{11} W/cm^2, for a cos^2 pulse with a FWHM of 20.3 fs. The energy of the photon is just above the ionization threshold and due to the ponderomotive upward shift of the continuum, the first full peak shown in the figure corresponds to a two-photon process. Note that the contribution of the ponderomotive shift to the width of the peak is negligible compared to the Fourier broadening. The successive widths of the peaks are 0.184 eV, 0.219 eV, 0.251 eV, 0.280 eV, 0.307 eV, 0.332 eV, 0.352 eV, and 0.375 eV, respectively, for processes of order 2, 3, 4, 5, 6, 7, 8, and 9. The bottom part of the figure shows the comparison of the peak-to-peak width
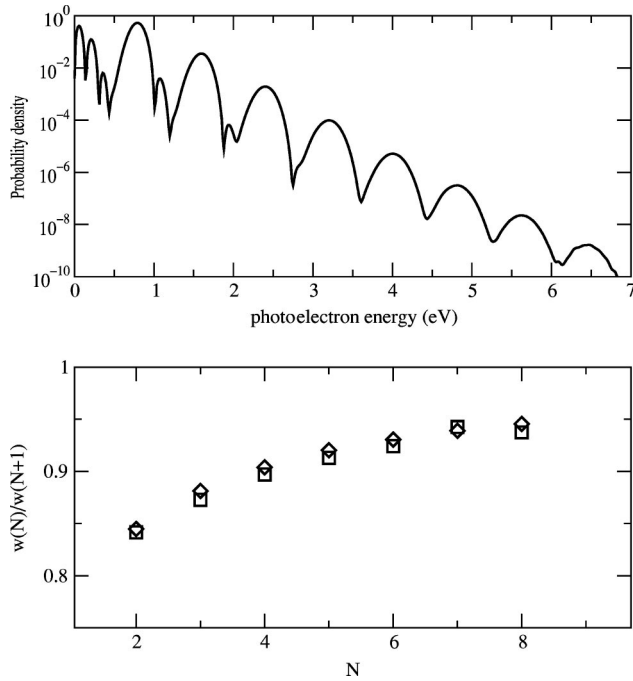
FIG. 2. The top figure shows the ATI spectrum (in eV^{-1}) of the negative hydrogen ion irradiated by a 20.3-fs pulse with peak intensity of 5×10^{11} W/cm^2 at 1519 nm. The bottom figure displays the ratio of the widths of successive ATI peaks. The square boxes are obtained from the calculated spectra and the diamonds are the values predicted by the model.

ratio predicted by the model to the ones of the numerical calculations, once again very good agreement is obtained.

In the second column of Table I we present the ratios of consecutive ATI peak widths as calculated for the cos^2 pulse profile according to our model. We used the field corresponding to the data shown in Fig. 2, but the main contribution to the result comes from the pulse profile and thus should be approximately correct for all cos^2 pulses. The values obtained from the data shown in Figs. 1 and 2 are shown in the

third and fourth column. We note that the variation due to the pulse shape is mostly seen in the lowest-order processes, and that the peak-to-peak difference gradually becomes less significant; however, there is a 5% effect even at the eighth-order processes. It should be noted here as an indicative example that the ratio of the width of the eighth-order peak to the first one is around 2.4. The parenthesis next to the numerical data show the absolute values of the relative errors compared to the results of the model. All numbers are well within 2% of those predicted by the model. The fifth column of Table I shows the value of the peak-to-peak ratios for a Gaussian-pulse profile. After the first-few peaks the ratios are very similar to the ones corresponding to the cos^2 profile. This trend of similarity toward the higher order of the process has its origin to the fact that the effective field $E^N(t)$ gradually looses information about the exact temporal shape of the fundamental field $E(t)$.

So far, we have presented our calculations on a specific atomic system, the negative hydrogen ion. The gradual broadening of the ATI peaks, however, is not restricted to any specific atomic system. It is a general feature of ATI spectra from Fourier-limited pulses, and in principle should be inherent in all such spectra. Cormier and Lambropoulos [12] presented the 0° ATI spectrum in Cs, using a 6-fs Gaussian pulse with peak intensity of 5×10^{10} W/cm^2 and wavelength of 620 nm, and have given the widths of the few lower peaks. The widths of the peaks corresponding to processes of order 3, 4, 5, are, respectively, 0.54 eV, 0.63 eV, and 0.7 eV. The relevant ratios are given in the last column of Table I and are in agreement with the model predictions for a Gaussian profile. All calculations that present ATI spectra using finite-pulse profiles should contain this feature.

Finally, to demonstrate the effect of ultrashort laser pulses in the photoelectron energy spectra of higher-order processes, consider the experiment performed by Walker et al. [27]. There they have used a 780-nm, 160-fs pulse for the single and double ionization of Helium. With this wavelength (1.59 eV), about 16 photons needed for the single

TABLE I. The ratios of the widths of successive ATI peaks corresponding to processes of order N. In parentheses the absolute value of the relative error of the calculation compared to the model is presented.

N	(cos^2)[a]	CI[b]	$w(N)/w(N+1)$ YM[c]	Gaussian[d]	CL[e]
1	0.776	0.761 (1.9%)		0.707	
2	0.845	0.831 (1.7%)	0.842 (0.4%)	0.816	
3	0.881	0.885 (0.4%)	0.873 (1.0%)	0.866	0.857 (1.0%)
4	0.904	0.911 (0.8%)	0.897 (0.8%)	0.894	0.900 (0.7%)
5	0.920	0.908 (1.3%)	0.913 (0.8%)	0.913	
6	0.930		0.924 (0.7%)	0.926	
7	0.939		0.943 (0.4%)	0.935	
8	0.945		0.937 (0.9%)	0.943	

[a]Model for a cos^2 pulse profile.
[b]CI basis calculation using a cos^2 pulse. Data taken from Fig. 1.
[c]Yukawa model B splines calculation using a cos^2 pulse. Data taken from Fig. 2.
[d]Analytical model for a Gaussian pulse profile.
[e]Cs calculations with a Gaussian pulse profile. Data taken from Cormier and Lambropoulos [1].

ionization while about 50 photons are needed for the double ionization. Modeling the pulse with a $\cos^2$ profile, we find for the effective-time interaction of an electron ejected with a N-photon absorption,

$$T_{\text{eff}}^{(N)} = \frac{(2N-1)!!}{(2N)!!} T, \qquad (8)$$

where, T is the total duration of the pulse. The spectral width of the Nth peak, will be approximately the inverse of this effective time $1/T_{\text{eff}}^{(N)}$. For the pulse adopted, spectral width is about $\Delta\omega = 4.11 \times 10^{-3}$ eV, which gives for the photoelectron energy width of the $N=20$ peak, about $2.6 \times \Delta\omega = 0.0105$ eV, a rather sharp peak, compared with the energy separation of the ATI peaks, which equals to the photon energy. Using, however, a pulse about one hundred times smaller in duration, ~1.6 fs, the latter number changes to $100 \times 0.0105 = 1.05$ eV, to be compared with the 1.59 eV of the photon frequency. It is obvious, therefore, that the peak structure of the photoelectron energy spectrum will disappear even in the first-few ATI peaks.

Finally, there are some experimental references that provide the widths of their ATI peaks, for example, the experiment of Nicklich et al. [28]. There the widths of the peaks corresponding to third- and fourth-order processes of ioniza-tion of Cs by a 70-fs pulse at 621 nm are shown for a range of intensities. Although there seems to be a qualitative agreement with our model for many of the measured widths we cannot make a definite statement since there may be more sources of broadening involved in the specific experiment than we have included in our model.

IV. SUMMARY

In summary, we have observed a gradual broadening of the successive ATI peaks in the Fourier-limited pulses. This feature has been attributed to the Fourier width corresponding to an effective pulse profile. For our simulations we have chosen the negative hydrogen ion, irradiated by 1064-nm and 1519-nm laser pulses. This system has the specific feature that its ATI peaks are free of resonance effects and the processes are of relatively low order thus making the features more pronounced. We believe that the gradual broadening of the peaks is a fundamental feature that is inherent in every ATI spectrum that is produced with Fourier-limited pulses.

[1] P. Lambropoulos, Phys. Rev. Lett. **55**, 2141 (1985).

[2] N. Papadogiannis et al., Phys. Rev. Lett. **83**, 4289 (1999).

[3] M. Drescher et al., Science **21**, 1923 (2001).

[4] P. Agostini et al., Phys. Rev. Lett. **42**, 1127 (1979).

[5] R. H. Freeman et al., Phys. Rev. Lett. **59**, 1092 (1987).

[6] D. Kim, S. Fournier, M. Saeed, and L. F. DiMauro, Phys. Rev. A **41**, 4966 (1990).

[7] J. Zhang and P. Lambropoulos, Phys. Rev. Lett. **77**, 2186 (1996).

[8] P. Lambropoulos, P. Maragakis, and J. Zhang, Phys. Rep. **305**, 203 (1998).

[9] D. Charalambidis et al., J. Phys. B **30**, 1467 (1997).

[10] C. J. G. J. Uiterwaal et al., Phys. Rev. A **57**, 392 (1998).

[11] J. N. Bardsley, A. Szöke, and M. J. Comella, J. Phys. B **21**, 3899 (1988).

[12] E. Cormier and P. Lambropoulos, Eur. Phys. J. D **2**, 15 (1998).

[13] S. Aseyev et al., AIP Conf. Proc. **525**, 399 (2000).

[14] X. M. Zhao et al., Phys. Rev. Lett. **78**, 1656 (1997).

[15] H. Andersen et al., Phys. Rev. Lett. **79**, 4770 (1997).

[16] L. Præstegaard, T. Andersen, and P. Balling, Phys. Rev. A **59**, R3154 (1999).

[17] M. Dörr et al., J. Phys. B **28**, 4481 (1995).

[18] D. A. Telnov and S.-I. Chu, J. Phys. B **28**, 2407 (1995).

[19] D. A. Telnov and S.-I. Chu, Phys. Rev. A **61**, 013408 (1999).

[20] L. A. A. Nikolopoulos and P. Lambropoulos, Phys. Rev. Lett. **82**, 3771 (1999).

[21] G. Lagmago-Kamta et al., J. Phys. B **34**, 857 (2001).

[22] T. N. Chang, in Many-body Theory of Atomic Structure, edited by T. N. Chang (World Scientific, Singapore, 1993), pp. 213–247.

[23] L. Collins and A. Merts, Phys. Rev. A **45**, 6615 (1992).

[24] C. Laughlin and S.-I. Chu, Phys. Rev. A **48**, 4654 (1993).

[25] P. Maragakis, E. Cormier, and P. Lambropoulos, Phys. Rev. A **60**, 4718 (1999).

[26] L. B. Madsen, L. A. A. Nikolopoulos, and P. Lambropoulos, Eur. Phys. J. D **10**, 67 (2000).

[27] B. Walker et al., Phys. Rev. Lett. **73**, 1227 (1994).

[28] W. Niklich et al., Phys. Rev. Lett. **69**, 3455 (1992).